Numerical Modeling of Geophysical Electromagnetic Inductive and Galvanic Phenomena

SeyedMasoud Ansari
Colin G. Farquharson

23 September, 2013

MEMORIAL
UNIVERSITY

Outline

1. Equations
   - E-field and Decomposed PDEs
2. Discretization
   - The minimization problem
   - Finite-Element functions
   - Solution to the system of Equations
3. Examples
   - Homogeneous half-space
   - Efficiency of the approach
   - Grounded wire and prism-in-half-space
   - Graphite cube in brine model
   - A marine example : Canonical disk model
4. Conclusions
5. Acknowledgments

Maxwell's equations

Deriving a PDE from Maxwell's equations, constitutive relations, Ohm's law in the quasi-static regime.

Faraday's law of induction

$$\nabla \times \mathbf{E} + i\omega\mu_0\mathbf{H} = \mathbf{0}, \tag{1}$$

Ampère's law

$$\nabla \times \mathbf{H} - \mathbf{J} = \mathbf{J}^s, \tag{2}$$

Ohm's law

$$\mathbf{J} = \sigma\mathbf{E} \tag{3}$$

$\mathbf{E}(\mathbf{r},\omega)$: Electric field, $\mathbf{H}(\mathbf{r},\omega)$: Magnetic field intensity, $\mathbf{J}^s(\mathbf{r},\omega)$: source current density, and $\sigma(r)$: Electrical conductivity

E-field PDE

$$\nabla \times \nabla \times \mathbf{E} \; + \; i\omega\mu_0\sigma\mathbf{E} \; = \; -i\omega\mu_0\mathbf{J}^s. \tag{4}$$

Because of the vanishing conductivity term, $i\omega\mu_0\sigma\mathbf{E}$ for lower frequencies it is difficult to solve the E-field equation.

- Decomposition of the electric field into potentials

$$\mathbf{E} = -i\omega\mathbf{A} - \nabla\phi \tag{5}$$

$\mathbf{A}(\mathbf{r}, \omega)$ and $\phi(\mathbf{r}, \omega)$ are vector and scalar potentials respectively.

$$\nabla \times \nabla \times \mathbf{A} \; + \; i\omega\mu_0\sigma\mathbf{A} \; + \; \mu_0\sigma\nabla\phi \; = \; \mu_0\mathbf{J}^s. \tag{6}$$

Equation of Conservation of Charge

For low frequencies also the coupling between **E** and **H** in the Maxwell's equations reduces and electric charges become important in distorting the field in the conductive medium.

$$\nabla \cdot (\sigma \mathbf{E}) = \begin{cases} -\nabla \cdot \mathbf{J}^s & \text{at the source location,} \\ 0 & \text{otherwise,} \end{cases} \tag{7}$$

Conservation of charge in the decomposed form

$$-i\omega \nabla \cdot (\sigma \mathbf{A}) \; - \; \nabla \cdot (\sigma \nabla \phi) \; = \; -\nabla \cdot \mathbf{J}^s. \tag{8}$$

Reiterating the Equations

The E-field system

$$\nabla \times \nabla \times \mathbf{E} \; + \; i\omega\mu_0\sigma\mathbf{E} \; = \; -i\omega\mu_0\mathbf{J}^s. \tag{9}$$

The Decomposed system

$$\nabla \times \nabla \times \mathbf{A} \; + \; i\omega\mu_0\sigma\mathbf{A} \; + \; \mu_0\sigma\nabla\phi \; = \; \mu_0\mathbf{J}^s, \tag{10}$$

$$-i\omega\nabla \cdot (\sigma\mathbf{A}) \; - \; \nabla \cdot (\sigma\nabla\phi) \; = \; -\nabla \cdot \mathbf{J}^s. \tag{11}$$

Introduction to discretization

Unstructured Tetrahedral meshes

Mesh generator tool: TetGen (Si, 2007)

Plotted using ParaView →

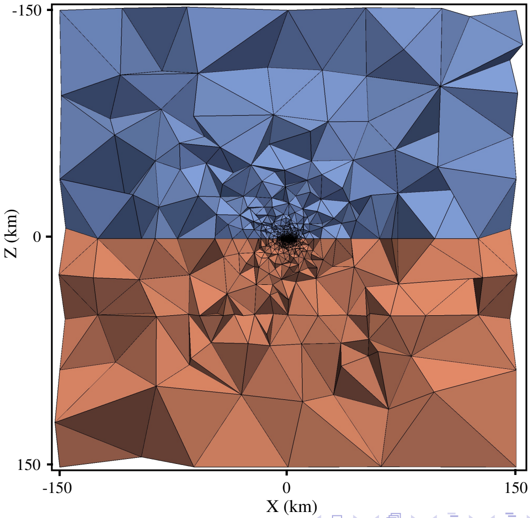

Working with unstructured meshes

Flexibility to optimally generate curvilinear contacts with minimal staircasing effects

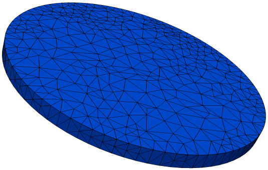

Only refining the mesh at the region of interest

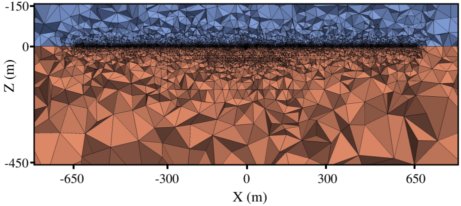

The method of weighted residuals

$$\mathrm{R} = \int_{\Omega} \mathbf{W} \cdot \mathbf{r} \; \mathrm{d}\Omega \; = \; 0, \tag{12}$$

with

$$\mathbf{r} = \nabla \times \nabla \times \tilde{\mathbf{A}} \; + \; i\omega\mu_0\sigma\tilde{\mathbf{A}} \; + \; \mu_0\sigma\nabla\tilde{\phi} \; - \mu_0\mathbf{J}^s.$$

$$\rho = \int_{\Omega} \mathrm{v} \; \mathrm{r} \; \mathrm{d}\Omega \; = \; 0, \tag{13}$$

with

$$\mathrm{r} = -\mathrm{i}\omega\nabla \cdot (\sigma\tilde{\mathbf{A}}) \; - \; \nabla \cdot (\sigma\nabla\tilde{\phi}) \; + \nabla \cdot \mathbf{J}^{\mathrm{s}}.$$

Finite-element basis functions

Vector basis functions or edge-elements for the approximate vector potential, $\tilde{\mathbf{A}}$

$$\tilde{\mathbf{A}} = \sum_{\mathrm{j}=1}^{\mathrm{n_A}} \tilde{\mathrm{A}}_{\mathrm{j}}\, \mathbf{N}_{\mathrm{j}}, \tag{14}$$

Scalar basis functions or nodal-elements for the approximate scalar potential, $\tilde{\phi}$

$$\tilde{\phi} = \sum_{\mathrm{k}=1}^{\mathrm{n}_\phi} \tilde{\phi}_{\mathrm{k}}\, \mathrm{N}_{\mathrm{k}}. \tag{15}$$

Linear Basis functions

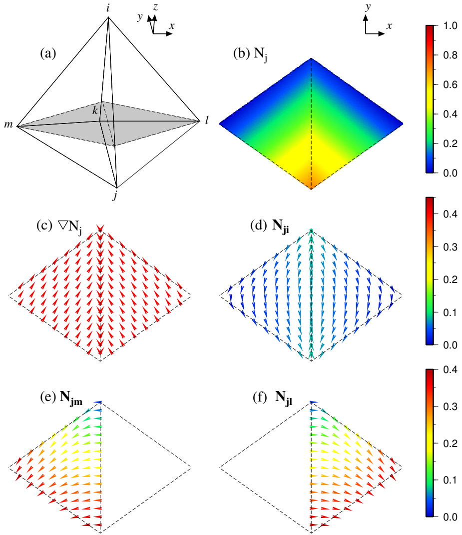

Weighted PDEs

$$\int_\Omega (\nabla \times \mathbf{W}) \cdot (\nabla \times \tilde{\mathbf{A}})\ d\Omega \ - \ \int_{\gamma+\Gamma} \mathbf{W} \times (\nabla \times \tilde{\mathbf{A}}) \cdot \hat{\mathrm{n}}\ dS \ + $$
$$\mathrm{i}\omega\mu_0 \int_\Omega \sigma\ \mathbf{W} \cdot \tilde{\mathbf{A}}\ d\Omega \ + \ \mu_0 \int_\Omega \sigma\ \mathbf{W} \cdot \nabla\tilde{\phi}\ d\Omega \ = \ \mu_0 \int_\Omega \mathbf{W} \cdot \mathbf{J}^{\mathrm{s}}\ d\Omega. \tag{16}$$

$$\mathrm{i}\omega \int_\Omega \nabla \mathrm{v} \cdot \sigma\tilde{\mathbf{A}}\ d\Omega \ - \ \mathrm{i}\omega \int_{\gamma+\Gamma} \mathrm{v}\ \sigma\tilde{\mathbf{A}} \cdot \hat{\mathbf{n}}\ dS \ + $$
$$\int_\Omega \nabla \mathrm{v} \cdot \sigma\nabla\tilde{\phi}\ d\Omega \ - \ \int_{\gamma+\Gamma} \mathrm{v}\ \sigma\nabla\tilde{\phi} \cdot \hat{\mathbf{n}}\ dS \ = \ -\int_\Omega \mathrm{v}\ \nabla \cdot \mathbf{J}^{\mathrm{s}}\ d\Omega. \tag{17}$$

Applying the Galerkin Method and Boundary conditions to the above ...

The $\mathbf{A} - \phi$ system in the matrix form

$$\begin{pmatrix} \mathbf{C} + \mathrm{i}\omega\mu_0\mathbf{D} & \mu_0\mathbf{F} \\ \mathrm{i}\omega\mathbf{G} & \mathbf{H} \end{pmatrix} \begin{pmatrix} \tilde{\mathrm{A}} \\ \tilde{\phi} \end{pmatrix} = \begin{pmatrix} \mu_0\mathrm{S}_1 \\ \mathrm{S}_2 \end{pmatrix} \tag{18}$$

Finite-element inner product functionals:
$\mathbf{C} = \mathcal{F}(\mathbf{N})$
$\mathbf{D} = \mathcal{F}(\sigma, \mathbf{N})$
$\mathbf{F} = \mathcal{F}(\sigma, \mathbf{N}, \nabla\mathrm{N})$
$\mathbf{G} = \mathcal{F}(\sigma, \mathbf{N}, \nabla\mathrm{N})$
$\mathbf{H} = \mathcal{F}(\sigma, \nabla\mathrm{N})$.

$\tilde{\mathrm{A}}$ and $\tilde{\phi}$ are the approximated potentials.

Source function

$$S_1 = \int_\Omega \mathbf{N}_i \cdot \mathbf{J}^s \, d\Omega \, , \qquad S_2 = -\int_\Omega N_l \, \nabla \cdot \mathbf{J}^s \, d\Omega.$$

Arbitrarily positioned in the mesh.

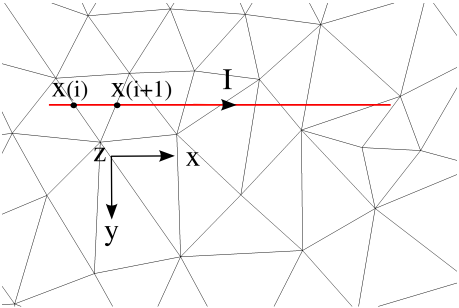

$$\mathbf{J} = I \, (\mathcal{H}(x_{i+1}) - \mathcal{H}(x_i)) \, \delta(y - y_0) \, \delta(z - z_0) \tag{19}$$

Iterative solution and preconditioning

$$\begin{pmatrix} \mathbf{C} + \mathrm{i}\omega\mu_0\mathbf{D} & \mu_0\mathbf{F} \\ \mathrm{i}\omega\mathbf{G} & \mathbf{H} \end{pmatrix} \begin{pmatrix} \tilde{\mathrm{A}} \\ \tilde{\phi} \end{pmatrix} = \begin{pmatrix} \mu_0\mathrm{S}_1 \\ \mathrm{S}_2 \end{pmatrix} \tag{20}$$

ILUT preconditioning (Saad, 1990) with an appropriate fill-in factor prior to solution

Iterative solver of GMRES from SPARSKIT (Saad, 1990): A generalized minimum residual method in the Krylov subspace

$$\tilde{\mathbf{E}} = -\mathrm{i}\omega\tilde{\mathbf{A}} - \nabla\tilde{\phi}$$

Inductive part: $-i\omega\tilde{\mathbf{A}}$
Galvanic part: $-\nabla\tilde{\phi}$

Frequency = 0.1 Hz, cells: 708796, nodes: 116058, edges: 825232. $\sigma_{\text{air}} = 10^{-8}$ S/m, $\sigma_{\text{Earth}} = 0.01$ S/m

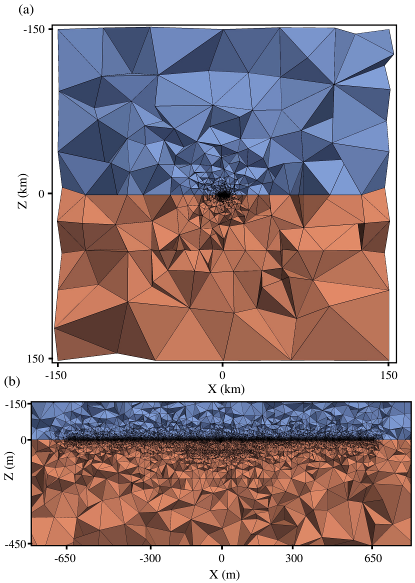

Electric dipole source

Comparison with the analytic total field solution.

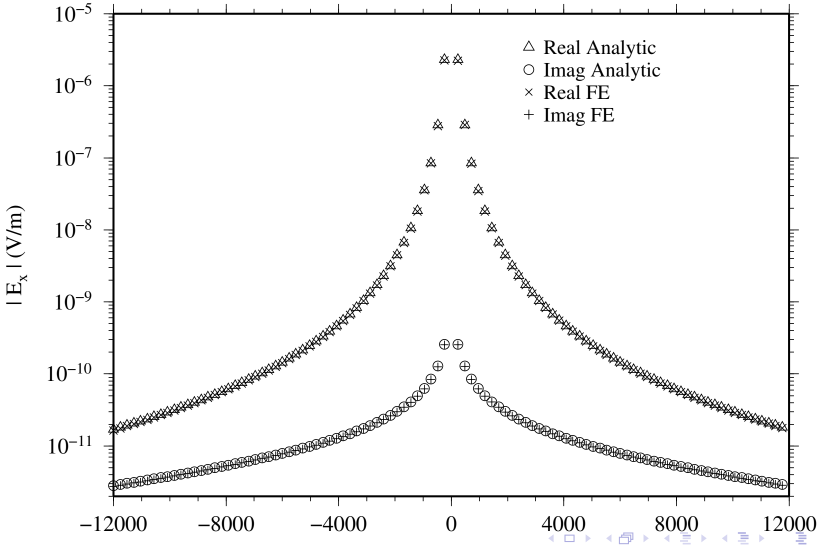

Solver parameters

GMRES solver, lfill = 3.
Dimension of the Krylov subspace: 200.
Residual norm of 10^{-12} after 4000 iterations.
Computation time for the solution was roughly 30 minutes on a Apple Mac Pro computer (2.4 GHz Quad-core Intel Xenon processor) with a total memory usage of 8 Gbytes.

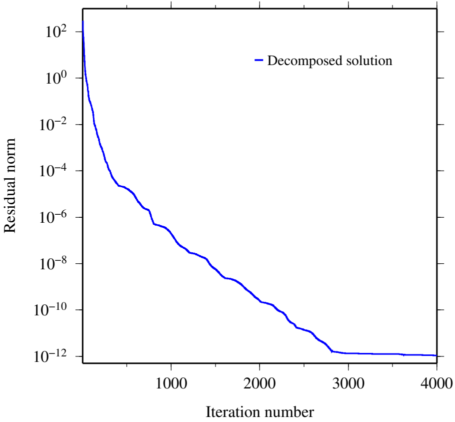

Inductive and Galvanic components

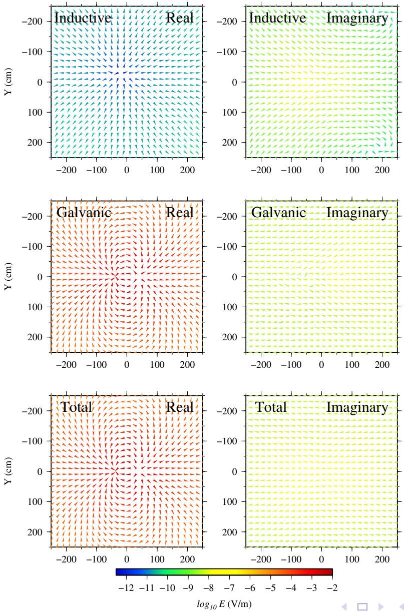

$\mathbf{A} - \phi$ solution against the E-field solution

The E-field system

$$\nabla \times \nabla \times \mathbf{E} \; + \; i\omega\mu_0\sigma\mathbf{E} \; = \; -i\omega\mu_0\mathbf{J}^s,$$

$$\begin{pmatrix} \mathbf{C} + \mathrm{i}\omega\mu_0\mathbf{D} \end{pmatrix} \begin{pmatrix} \tilde{\mathrm{E}} \end{pmatrix} = \begin{pmatrix} \mathrm{i}\omega\mu_0\mathrm{S}_1 \end{pmatrix} \quad (21)$$

The $\mathbf{A} - \phi$ system

$$\begin{pmatrix} \mathbf{C} + \mathrm{i}\omega\mu_0\mathbf{D} & \mu_0\mathbf{F} \\ \mathrm{i}\omega\mathbf{G} & \mathbf{H} \end{pmatrix} \begin{pmatrix} \tilde{\mathrm{A}} \\ \tilde{\phi} \end{pmatrix} = \begin{pmatrix} \mu_0\mathrm{S}_1 \\ \mathrm{S}_2 \end{pmatrix} \quad (22)$$

Magnetic dipole source

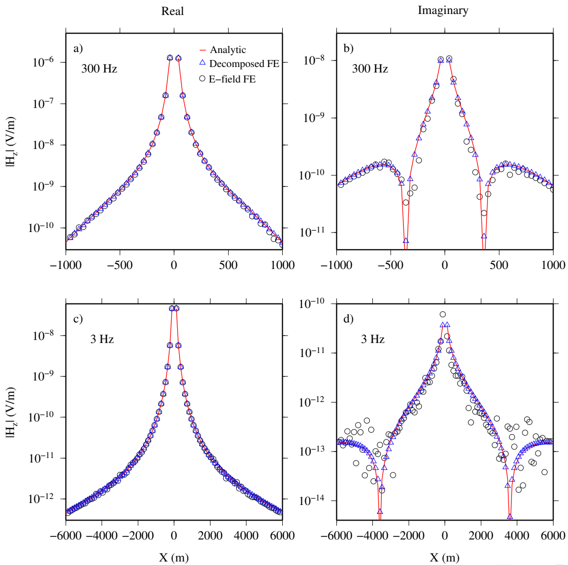

Residual norms

Rapid convergence of the $\mathbf{A} - \phi$ solution

Slow convergence of the E-field solution

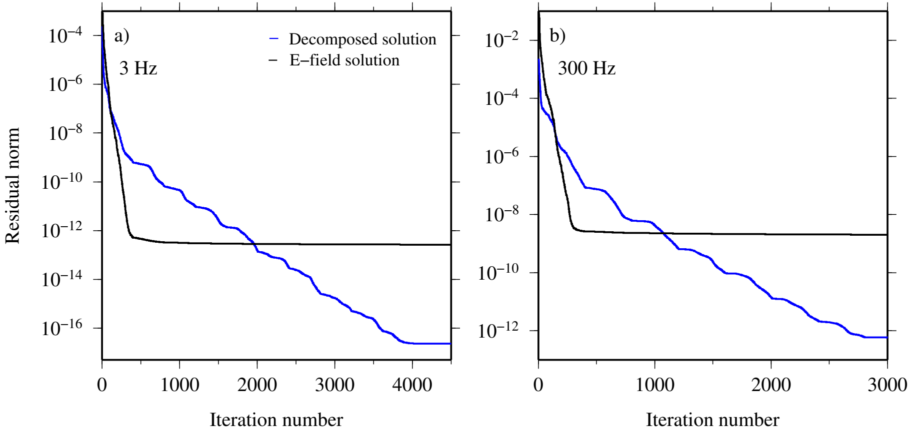

Grounded wire and prism

A mineral exploration scenario done by Li, Oldenburg and Shekhtman, 1999 : DCIP3D
Farquharson and Oldenburg, 2002 : Verification of the Integral Equation code
Frequency = 3 Hz

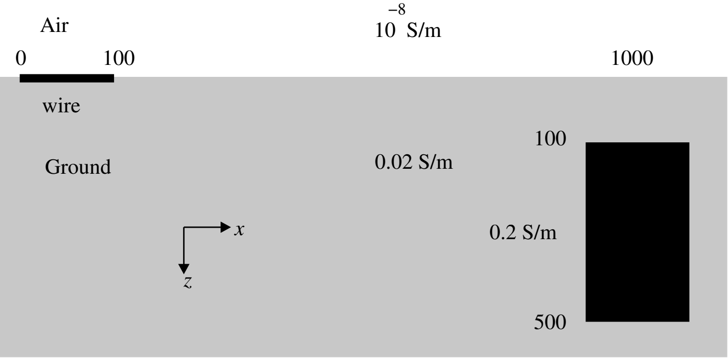

Unstructured Mesh

cells: 613300, nodes: 99855, and edges: 713542

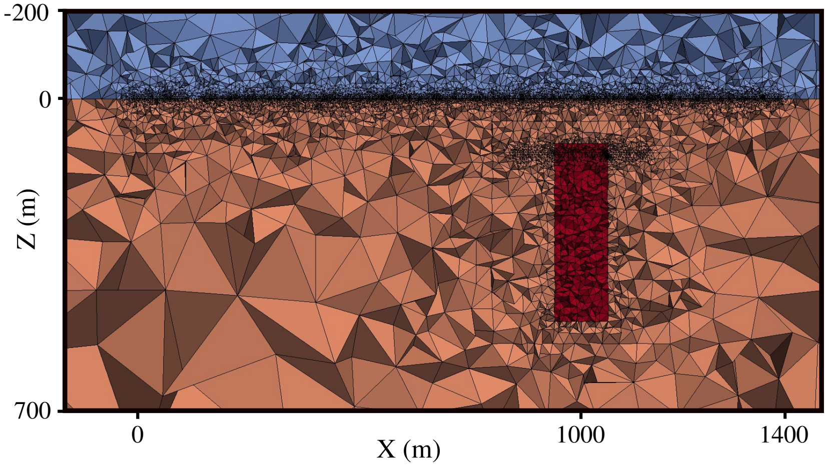

Electric fields

Comparison against Integral Equations and DC-resistivities.

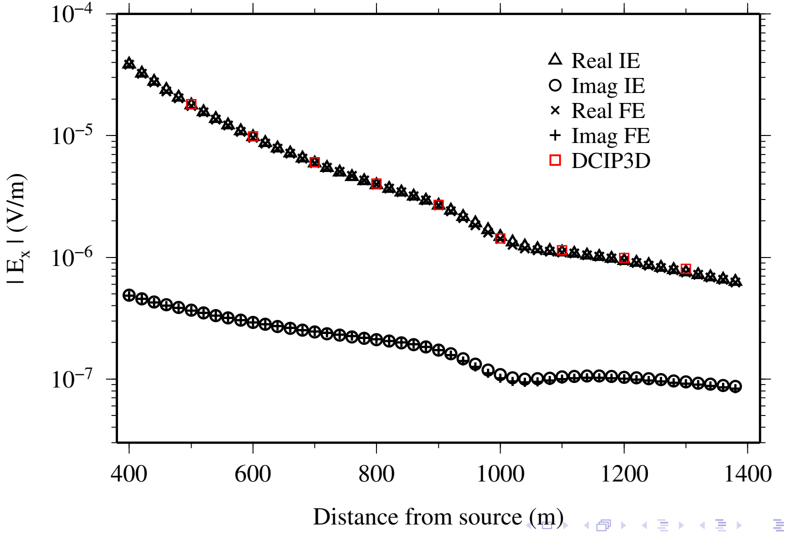

Scattered fields

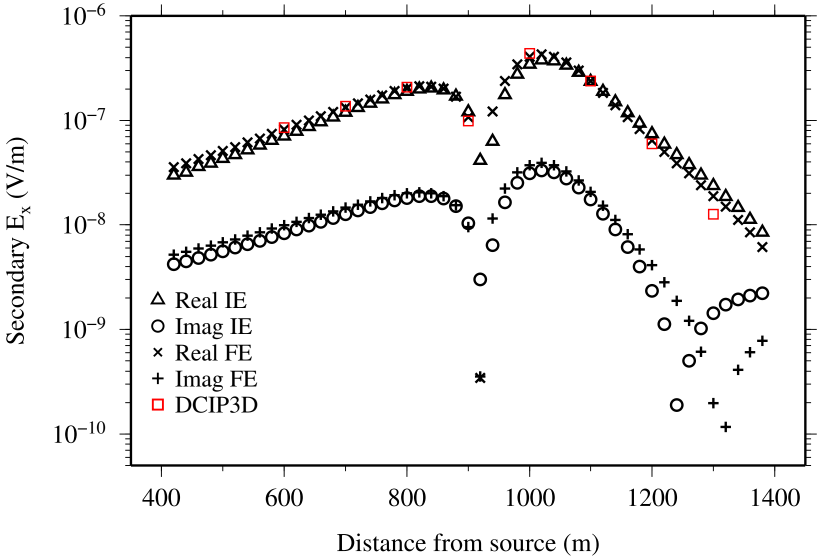

Inductive and Galvanic fields

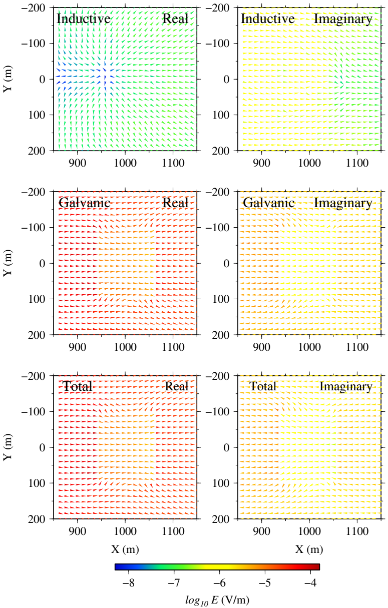

Inductive and Galvanic current density

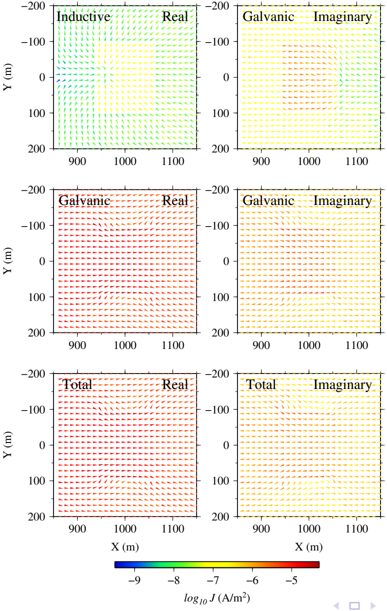

Transmitter-Receiver pair and cube in brine

Comparison against the physical scale modeling of Farquharson et al., 2006 and Finite-volume solution of Jahandari and Farquharson, 2013.

Five frequencies 1, 10, 100, 200, and 400 kHz.

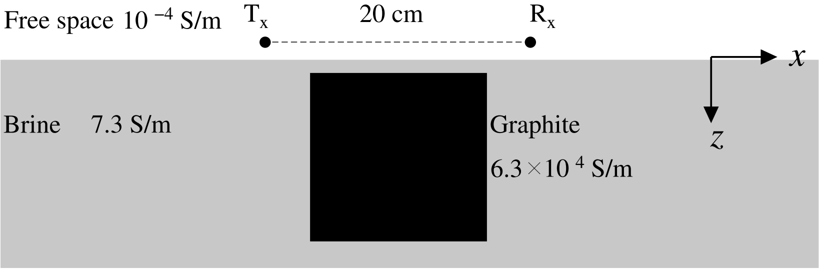

Unstructured Mesh

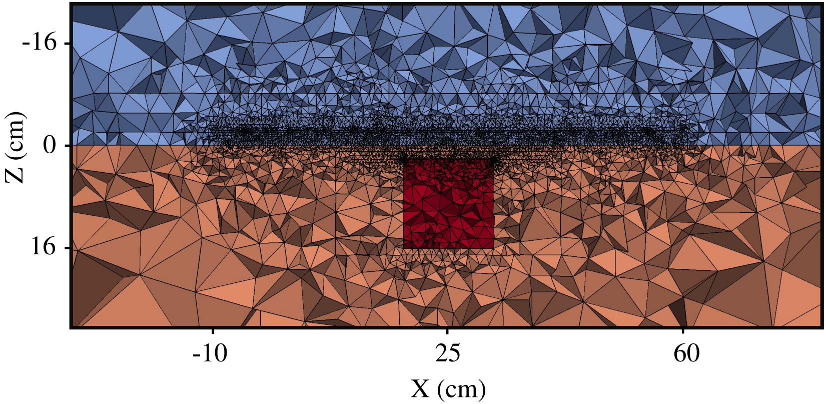

Normalized magnetic fields: FE, FV, Physical Scale modeling

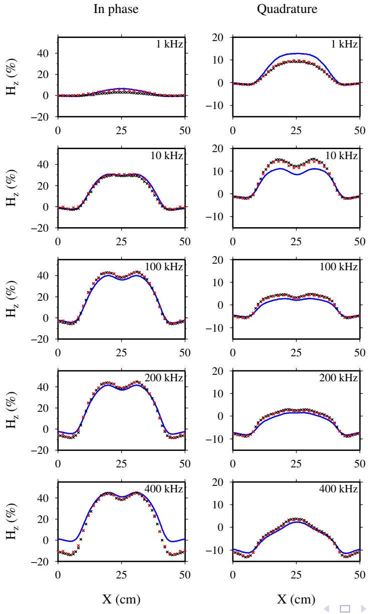

Inductive and Galvanic fields

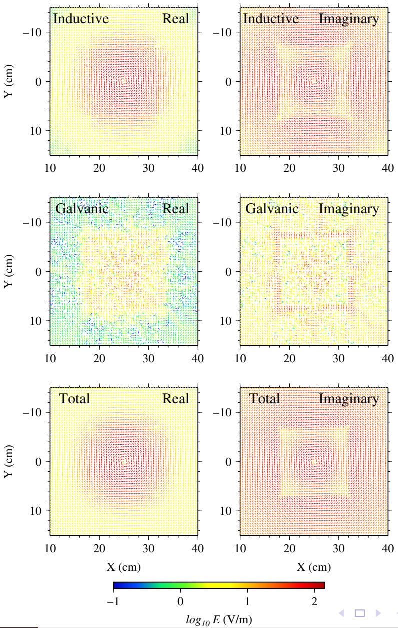

Inductive and Galvanic current densities

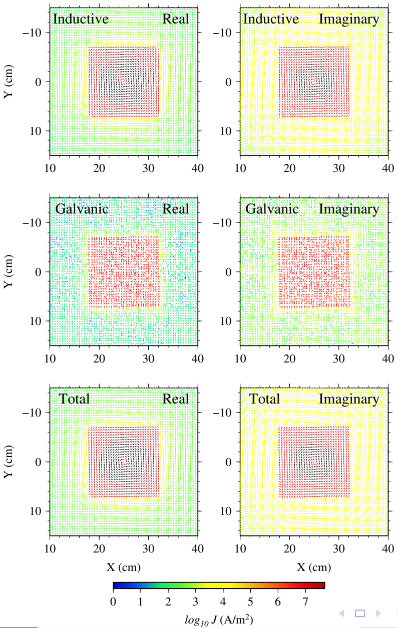

Canonical disk model in marine sediments

A hydrocarbon exploration scenario by Constable and Weiss (2006)

Frequency of 1 Hz

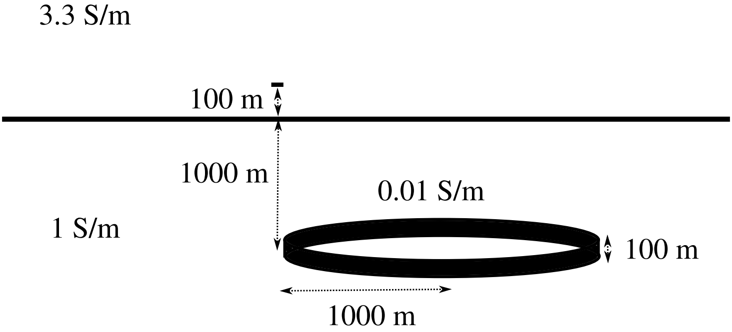

In-line total electric fields.

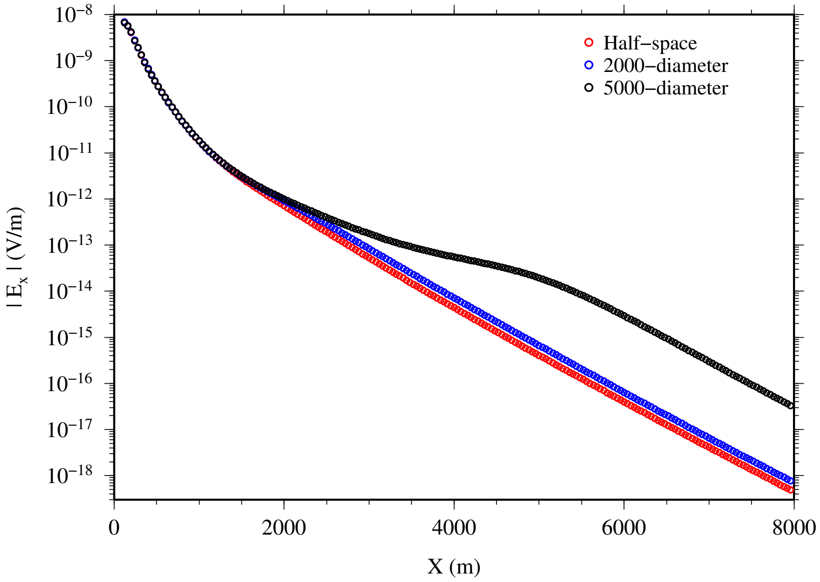

In-line total electric fields.

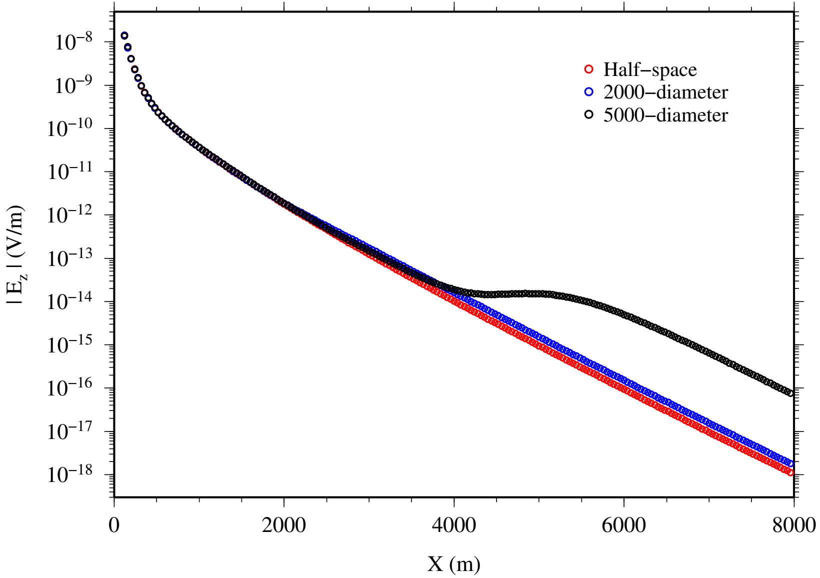

In-line total electric fields.

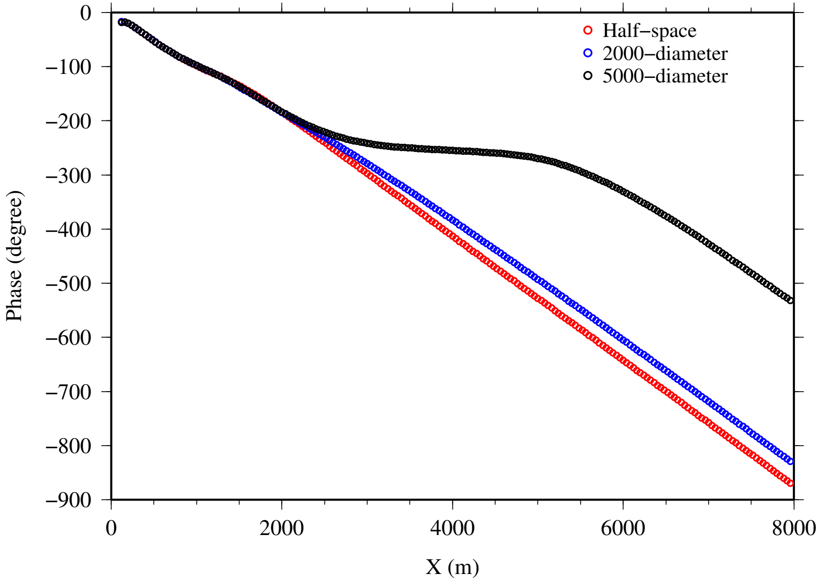

Inductive and Galvanic fields

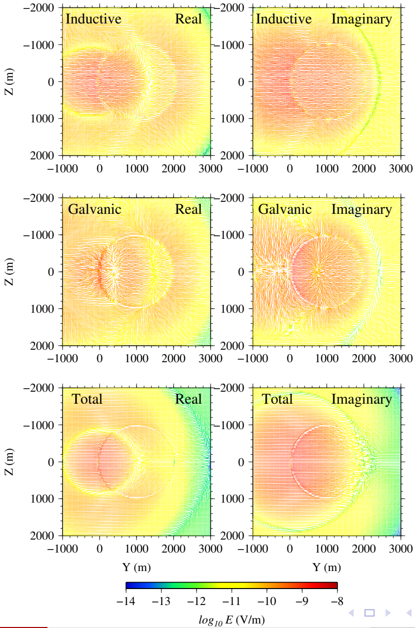

Inductive and Galvanic current densities

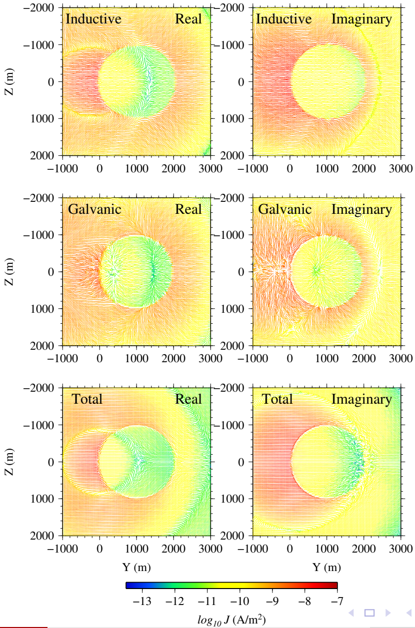

Conclusions

- A 3D finite-element solution for forward modeling of geophysical electromagnetic problems is presented.
- The algorithm is written for the total field approximation on unstructured tetrahedral meshes.
- The approach is based on decomposing the electric field into vector and scalar potentials in the Helmholtz equation and equation of conservation of charge.
- The decomposition is done not only from the perspective of solving the equations efficiently, but also in order to delve into the physical meaning of the inductive and galvanic components.
- We verified the method for multiple examples in different geophysical scenarios where either electric and magnetic sources are used.

Acknowledgments

Dr. Peter Lelièvre

For providing auxiliary subroutines for unstructured meshes.